Electromyographic Classification to Control the SPAR Glove ⋆

John E. Britt * **Marcia K. O'Malley** * **Chad G. Rose** **

* *Department of Mechanical Engineering, Rice University, Houston, TX, USA (e-mail: omalleym@rice.edu).*
** *Department of Mechanical Engineering, Auburn University, Auburn, AL, USA (e-mail:chadgrose@auburn.edu)*

Abstract: The SeptaPose Assistive and Rehabilitative (SPAR) Glove has been developed to assist individuals with upper extremity impairment arising from neuromuscular injury. The glove detects user intent via the MYO wearable electromyography (EMG) device. In this manuscript, pattern recognition tools infer the desired hand pose from EMG activity. The ability of the measurement and classification methods to distinguish between hand poses was evaluated with nine able-bodied participants and three participants with spinal cord injury (SCI) in an offline experiment. The strong performance of the proposed intent detection method is shown in the steady-state classification accuracy, presented as confusion matrices, as well as the average confidence for each classification. Building upon the strong performance in detecting pose, a pilot study with two participants with SCI presents the initial results of the real-time implementation of the system, which suggests directions for future work in improving the steady-state classification accuracy through expanded measurement and a refined taxonomy to enable intuitive control.

Keywords: Assistive and Rehabilitation Robotics; Robotics; Machine Learning in modeling, estimation, and control

1. INTRODUCTION

Each year approximately 17,000 people experience a spinal cord injury (SCI) that impairs motor function (National Spinal Cord Injury Statistical Center (2017)). Many of these individuals retain some ability to move their upper extremities but lack the strength to produce enough movement to complete tasks associated with activities of daily living (ADL). Assistive devices have the potential to help these individuals regain functional independence by increasing the strength and dexterity of the hand. Surveys of SCI participants confirm that such an increase in dexterity would represent a significant increase in their quality of life (QOL), as 71% of people with tetraplegia require assistance with ADL (Collinger et al. (2013)). With improved hand function and independence, people who have suffered an SCI can seek employment, improving their finances as well as their participation in their communities, resulting in improved QOL (Dijkers (1997)).

Assistive devices may also contribute to improved *rehabilitation* outcomes for those with incomplete SCI, by providing support for functional tasks that might in turn result in increased use of the impaired limbs. Many individuals undergo physical therapy following SCI, and this has proven effective at increasing neuro-plasticity reward (Edgerton et al. (2004)). Evidence has shown that high-intensity and repetitive practice can lead to recovery of some spinal cord, and therefore extremity, function (Dietz et al. (2002)). Further, functional training has shown to have beneficial effects in promoting spinal plasticity which can help lead to recovery (Dietz and Fouad (2014)).

Assistive devices, particularly those compatible with at-home use, may be uniquely suited to increase functional training. Incorporating functional tasks has been shown to be beneficial in the rehabilitation of stroke survivors, and it is reasonable to expect that the same would hold true for individuals with SCI (Kristensen et al. (2011)). This expectation is supported by animal model studies (Cai et al. (2006)). Performance of ADL with an assistive device provides a useful platform for physical therapy and helps the participant enhance skills that directly improve their QOL. Frequent usage of therapeutic assistive devices has the potential to create a feedback loop wherein frequent use improves ability and increased ability results in more frequent use (Winstein et al. (1999)). Despite evidence of motor function improvement with the 120 devices surveyed by Maciejasz et al. (2014), the ability to perform ADL was not enhanced any more than conventional therapies. This opens up a window for development of a device that specifically addresses ADL movements.

1.1 Capabilities to Assist Hand Function

Devices for hand assistance should consider the poses that most contribute ADL. For example, Dollar (2014) catalogued a comprehensive set of grasps involved in ADL. In related work, Dalley et al. (2011) identified a set of seven

⋆ This work was supported by NASA Space Technology Research Fellowship (NSTRF, NNX13AM70H); Rice University IDEA Grant; Mission Connect, a project of the TIRR Foundation (015-103, 017-102); and the Rice Global Engineering and Construction Forum.

poses, shown in Fig. 1, that are necessary to accomplish most ADL, and used them for the control of a prosthesis.

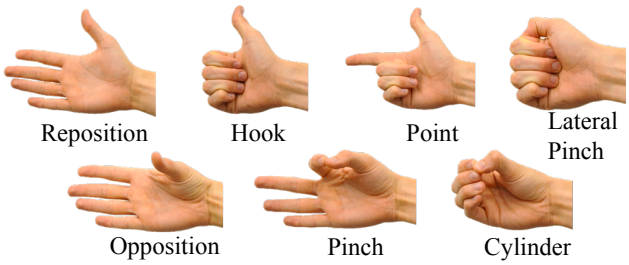

Fig. 1. The taxonomy proposed by Dalley et al. (2011) consists of seven hand poses critical to accomplishing the majority of ADL. This set of poses served as the basis for a myoelectric prosthetic control scheme.

1.2 Detecting User Intent for Assistive Device Control

Intent detection, as defined by Losey et al. (2018), is the passing of information about the human planned action to a robot through a defined channel of communication. Led by the prosthetic community, most commercial devices opt for myoelectric or body-powered control (Fougner et al. (2012)), with advanced brain machine interfaces (BMI) largely remaining in the lab (Shanechi (2017)). Common implementations of intent detection for orthoses are coupling between less-impaired joints and electromyography (EMG) control, similar to body-powered control and myoelectric (EMG) prostheses, respectively (Chu and Patterson (2018)). Typically, these control schemes use dichotomous open/close architecture. Of the 44 devices reviewed by Chu and Patterson (2018), only 13 presented a form of intent detection broadly categorized into manual selection, kinematic couplings, and EMG.

Manual selection, relying on the user to operate switches or buttons, such as the system proposed for HES by Conti et al. (2017), or voice commands (Triandafilou et al. (2011)) trade unobtrusiveness for ease of operation and unequivocal intent detection. The Exo-Glove (In et al. (2015); Jeong et al. (2013)) implemented bend sensors at the wrist to control grasp aperture, following the kinematic coupling between the wrist and fingers known as the tenodesis grasp (Johanson and Murray (2002)). EMG control of wearables is rapidly becoming standard, following developments in the prosthetics community (Fougner et al. (2012)), particularly with strategies for overcoming underactuation and taxonomy-based designs (Santello et al. (1998)). Designs such as J-Glove (Ochoa et al. (2011)) use EMG to detect intent and promote engagement, where a certain EMG activation thresholds must be overcome before the motor will move in 10% increments. Many devices detect EMG activation across a predefined window, and return force based on the the proportion of the current signal to maximum voluntary effort, as implemented on cable driven (Delph et al. (2013)), and pneumatic devices (Polygerinos et al. (2015)). The work of Kadowaki et al. (2011) sought to discriminate between wrist and finger activity, but also limited command to flexion and extension of a single DOF. Dwivedi et al. (2019) commanded multiple poses to a device, but the poses were predetermined with the EMG serving only as a trigger for the selected pose.

However, EMG is capable of providing more granular information beyond dichotomous open/close architectures, down to digit and hand pose. McDonald et al. (2020) incorporated EMG into a control scheme for an upper arm device to detect wrist and forearm intent. To improve intent detection in prosthetics, Mendez et al. (2017) sought to evaluate the MYO EMG armband for its ability to distinguish hand poses, and Gailey et al. (2017) used an array of EMG electrodes, with some arbitrary and some targeted muscle location placement. However, there have been limited studies into the feasibility of using low-cost EMG measurement arrays to detect residual muscle activations in impaired individuals.

1.3 Contributions

In the work by Rose and O'Malley (2019), keystrokes controlled the velocities of the motors acting in opposing motions of flexion and extension to move individual fingers as needed, which was sufficient for demonstrating basic efficacy of the SPAR Glove. To further investigate the glove's potential for assisting with ADL, the ability to command multiple desired poses in an intuitive manner is necessary. It is the goal of this manuscript to validate a proposed intent detection scheme that uses the commercially available MYO armband as a low-cost wearable intent detection device for the requisite poses of the SPAR Glove. Whereas the use of EMG has been largely limited to simple agonist/antagonist pairs, as in the works of Cao and Zhang (2016) as well as Delph et al. (2013), this work seeks to generalize the use of EMG to distinguish between seven different poses which have been identified as useful for ADL. The outstanding question surrounding use of the SPAR Glove addressed by this manuscript is whether intent detection of the proposed grasp taxonomy is feasible using EMG with the SCI population.

To determine the feasibility of the proposed intent detection system introduced in Section 2, a validation experiment, discussed in Section 3.2, was performed with both able-bodied and SCI participants. Participants wore the MYO EMG armband as they performed the goal poses to evaluate the steady-state classification accuracy of the intent detection algorithm operating in an offline mode. Motivated by the results of the validation experiment, a pilot study, discussed in 3.3, was conducted to evaluate real-time classifier accuracy. The results of the validation experiment and pilot study are presented in Section 4 and discussed in Section 5, before the manuscript's contributions are summarized in Section 6.

2. ELECTROMYOGRAPHIC INTENT DETECTION

The glove uses seven linear actuators (BLDC, Maxon 405794), planetary gear (4.4:1) and ball screw transmission (2 mm pitch, Maxon 424222)), to retract tendons routed through Bowden cable transmissions. The resulting motions of the actuated degrees of freedom (DOF) allow the SPAR Glove, shown in Fig. 2, to achieve seven distinct poses proposed by Dalley et al. (2011) and shown in Fig. 1 as those necessary to achieve a large portion of ADL. To detect user intent, the SPAR Glove uses the MYO, a commercial-off-the-shelf EMG devices with 8 electrodes.

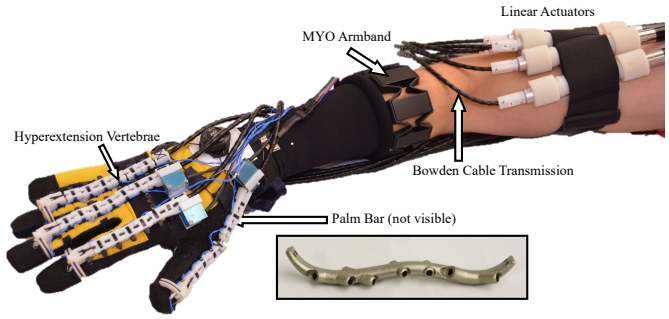

Fig. 2. The SeptaPose Assistive and Rehabilitative (SPAR) Glove first proposed by Rose and O'Malley (2019) assists the seven pose taxonomy identified by Dalley et al. (2011). The intended pose of the wearer is identified by classifying EMG signals captured by the MYO Armband. Further intent detection is possible through the use of bend sensors located at the wrist.

2.1 Low-Level Control of the SPAR Glove

The position of each actuator's ball screw is governed by a PD controller, which is enables straightforward tuning of the response of the tendon not available with P control. The setpoints are defined in terms of the carriage positions along the lead screws and are commanded via a gearbox ratio defined within custom software developed at Rice University, the Mechatronics Engine & Library (Pezent and McDonald (2019)). In the current implementation, the commanded positions for each motor are selected from a table of setpoints based on the desired pose. When the command to move to a particular pose is sent, the setpoint for each motor is changed to reflect the motor's desired position in the applicable pose.

2.2 User Interface for Control

To convert the EMG signals captured by the MYO armband, the SPAR Glove uses a Linear Discriminant Analysis method that is based on the work of McDonald et al. (2020). In that work, researchers placed EMG sensors placed directly over the muscle bellies to control a rehabilitation robot. The MYO armband works on a different principle, relying on an array to capture activity, without precise muscle placement. The proposed algorithm computes a set of features from EMG data based on the foundational work of Hudgins et al. (1993). Those features are: the number of zero crossings (ZC), mean absolute value (MAV), waveform length (WL), number of slope sign changes, four coefficients (AR1, AR2, AR3, and AR4) of a fourth-order autoregressive model, and root mean square (RMS). The proposed algorithm computes these nine features for each of the eight EMG channels of the MYO to build a classifier unique to training data. Note that while the features are unique to each trained set, the weightings of these parameters were fixed for the experiments in this manuscript. This general functionality was built into the Mechatronics Engine & Library Pezent and McDonald (2019). The algorithm is intended to be trained before each use, to account for differences in placement of sensors after donning the MYO. In the current implementation, training takes approximately 7 minutes (for more details, see Section 3.2).

The output of the classifier developed by McDonald can be utilized to represent the poses the wearer is intending. While the classifier can examine a moving window of data and issue a prediction, to improve the performance of the intent detection, the algorithm must cross a threshold number of predictions that must be reached prior to the device being actuated. The current implementation of the intent detection algorithm has a 1 second (1000 predictions) threshold that must be crossed prior to actuation. This introduces delay, since an imperfect classifier will always take longer than 1 second to generate enough correct predictions to cross the threshold, but the increased reliability of the final movement is more important when interacting with objects in the physical world.

3. VALIDATION OF INTENT DETECTION

An experiment, described in Section 3.2, sought to determine whether the data generated by the MYO EMG armband is of sufficient quality to be reliably classified between the 7 goal poses. To separate any limitations arising from real-time implementation, this experiment classified data offline. A pilot study, described in Section 3.3, explored whether the performance with the carefully segmented data from the validation experiment will translate to accurate classifications of live data.

3.1 Participants

The validation experiment collected data from both able-bodied participants and individuals with SCI, while the pilot study was done with SCI participants only. The able-bodied participants were all right handed and ranged in age from 22 to 35 years old. Three SCI participants, male, ranged in age between 42 and 65 years old, and right-handed prior to injury performed the validation experiment. Only the second and third SCI participants participated in the pilot study. All data collection was undertaken in compliance with the recommendations of the Rice University IRB, protocol 882515-1, with written informed consent obtained from all participants.

Initial testing showed that the task caused the MYO to shift on some of the participants' arms, particularly those with muscle atrophy. Since the classifier is sensitive to changes of electrode placement, the participants donned a compression wrap over the MYO.

3.2 Offline Classifier Accuracy

To determine whether the classifier can be used to successfully discriminate between the 7 goal poses, test participants were recruited to cycle their hands through the various goal poses and hold those poses for 4 seconds. The data were then parsed to isolate segments of data to be used to train the classifier. Each participant listened to a recorded set of instructions directing them to hold a particular goal pose for four seconds, then relax for two seconds in a neutral position before being given the next pose cue. Each participant performed each pose in this manner for 10 repetitions.

The samples generated during data collection were parsed so that the time-series data showing muscle activation were

separated from the data showing relaxation. To separate the different pose-generation sequences, the root mean square (RMS) of the raw time domain muscle activations were segmented with crossing a 10% threshold of max RMS identified as potential start points. All eight EMG channels were segmented based on the channel that had the most even segmentation, that is, the largest minimum gap between these 10% threshold crossings. Once the "best" channel was determined, the edge placements were applied to all channels and data could be parsed into segments for use in the classifier. The data were then separated into a series of training and evaluation data sets. These sets consisted of every unique combination of seven sets of training data, with the remaining sequences classified.

3.3 Pilot Study: Online Classifier Accuracy

To expand on the validation experiment, a pilot study was conducted to explore the performance of the classifier in a real time implementation. As in the validation experiment, the classifier was provided with seven segmented samples for training each pose. However, the training set was manually captured in real time prior to this experiment, and not segmented in a post-processing stage in a similar manner to the validation experiment. Instead of the four second pose and two second rest periods from the validation experiment, the pilot study participants stepped through the seven goal poses, holding each pose for ten seconds before resting and moving to the next pose. Participants were not notified of the classifier's output, to separate the wearer's ability to modulate in response to biofeedback from the intent detection algorithm.

4. RESULTS

The results of the validation experiment and pilot study show that the EMG signals captured by the MYO armband possess enough information to classify the seven goal poses, but there are still some limitations to the intent detection algorithm, especially for real-time implementation.

4.1 Offline Classification results

First, the measurements from the MYO are sufficient to classify the seven goal poses, as shown by the average confusion matrix for able-bodied participants in Fig. 3. The results for the three participants with SCI are shown in Fig. 4. These results show similar performance to the able-bodied participants, but with some decreased classification accuracy for poses which are mainly differentiated by thumb position, such as the lateral pinch and hook.

An additional metric beyond the classification accuracy to consider is the confidence rating presented by the intent detection algorithm. This confidence represents the 'distance' between the classes, which increases the more separable the different classes are, normalized from 0-100%. The classifier selects the class with the highest confidence, and the accuracy of this selection is described in Fig. 3 and 4. The algorithm's confidence in its classification can further explain the quality of the classification. These confidence values for able bodied subjects are presented in Fig. 5, which shows the confidence ratings for each

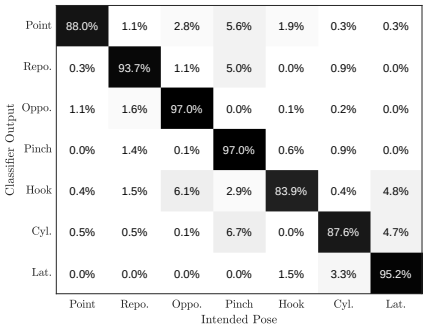

Fig. 3. Average confusion matrix for the offline classification of able-bodied participants' EMG activations, with intended pose on the horizontal axis, and classifier's output on the vertical. High values along the diagonal show strong performance for nearly all poses.

classification averaged across able-bodied participants. Of particular note is that the main diagonal's average confidences are typically near 90%, whereas the off-diagonal (incorrect) classifications hover closer to 50%, indicating that the classifier can indicate to the wearer and device that the classification is likely to be incorrect.

The average confidence values for the SCI participants are presented in Fig. 6. These results show high confidence for the first SCI participant, but decreased confidence values for the other two. Still, the diagonal (correct) classes typically had the highest confidences, further supporting the ability of our procedure to acquire data from the MYO and rely on the classifier to separate the EMG data into recognizable end goal poses.

4.2 Pilot Real-Time Results

The results of the real-time tests for SCI participant 2 and 3 are shown in Fig. 7. These values in the matrix reflect the percentage of the ten second period during which the classifier correctly identified the intended pose through the previously described threshold method.

5. DISCUSSION

The results from the validation experiment and pilot study suggest that the MYO and the proposed EMG classification algorithm are capable of detecting user intent and accurately selecting the goal pose.

5.1 Offline classification with able-bodied participants

From the results it is clear that the majority of classifications in able-bodied participants are unambiguous when the data is carefully chosen, though not all poses are equally clear. For example, the poses which are only differentiated by thumb opposition, such as the cylindrical grasp and the lateral pinch, are sometimes incorrectly classified as the other. Note that in the confidence values shown in Fig. 5, during the 5% of the trials where lateral pinch was incorrectly classified were above 70%. The confidence values for all poses, and these poses in particular, suggest a few interpretations. While it is possible that the particular training data used was insufficient to train the algorithm to

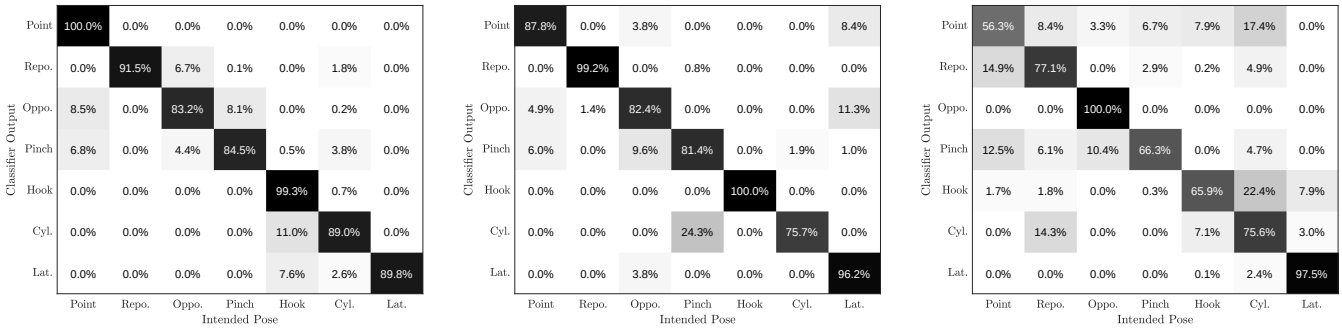

Fig. 4. Confusion Matrices for the offline classification of SCI participants (1-3, from left to right), with intended pose on the horizontal axis and classified pose on the vertical axis. The high values along the diagonal show similar performance to the able-bodied participants. However, certain poses which are mainly differentiated by thumb opposition, such as the hook, cylindrical grasp, and lateral pinch, had lower performance.

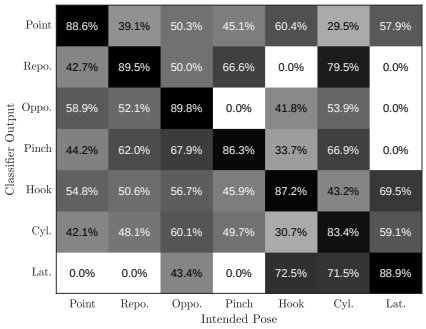

Fig. 5. Average confidence values for each classification for the offline classification of able-bodied participants' EMG activations. The high values along the diagonal are a representation of the separability of the trained classes and the classified data, which supports the use of the MYO and intent detection algorithm to classify the seven goal poses using forearm EMG.

separate the different classes, the other, more successfully-separated classes with high average confidences suggests that this is not the case. Another interpretation is that the muscle activations which control the thumb are not well captured by the MYO. To improve the performance of this intent detection method, there are a few options. First, we could seek to increase the confidence with an additional EMG sensor at the thenar eminence to capture activations of the abductor pollicis brevis detect thumb opposition activations. Second, the use of monopolar electrodes (as opposed to the MYO's bipolar electrodes (Xu et al. (2020))), could improve measurement of the contribution of deep muscles (Piovanelli et al. (2020)). Third, we could expand the algorithm to include input from another type of sensor, such as one of the bend sensors in the wrist, or another modality such as IMU to better predict the desired pose (Bennett and Goldfarb (2017)). Fourth, we could reconsider the goal poses, and instead of trying exert effort to discern the difference between similar poses, focus on identifying other key aspects of the poses or different poses all together. Perhaps these poses, which were used to explore the DOF space are not well separable in the muscle activation space, and it would be more reasonable to train on a related, but slightly different taxonomy. The end goal would be to create a more separable set of activations which can control the glove. Such a set could consider activations to classify the four DOF from the original use of the taxonomy by Dalley et al. (2011), or even a more reduced set, relying on more passive constructions to open and close the fingers. Perhaps the easiest, and most robust option would be to have the algorithm consider its confidence when making decisions, and when the confidence is below a specified threshold, request confirmation or some other secondary 'check' on the intent detection.

5.2 Offline classification with SCI participants

The classifications in SCI participants were more ambiguous than those of able-bodied participants. Some participants were unable to command their hands into the desired poses, but were still able to generate some muscle activations. Even with the reduced magnitude and quality of muscle activations, the confusion matrices generated by the classifications of SCI participants' activations demonstrates that classification is possible using only the EMG data from the MYO armband. Of note is the relatively higher performance of certain poses, such as the Hook pose, in the participants with SCI than in the unimpaired participants, both in terms of the confusion (accuracy) matrix and reported confidence values. Increased resolution in the muscle activations associated with thumb movement may explain this point of interest.

5.3 Real-time performance of intent detection algorithm

The reduced performance in the pilot study could be the result of a few factors. First, while the training data was of the same type as in the validation experiment, the evaluated data was changed for the pilot study to a 10 second stream to allow the classifier to make a series of predictions. While there is likely a difference between activations generated while initiating a pose from rest from those generated by holding a certain pose for able-bodied individuals, it is not clear if the same is true for impaired individuals who never reach the desired pose. It is also possible that the 'first-past-the-post' interpretation of the classifier output along with the lack of feedback provided to participants contributed to some of the decrease in performance. In addition to feedback, further training with the MYO beyond the 15 minutes in this study could have improved performance. Lastly, the manually-captured training data, expected to be similar to a real-

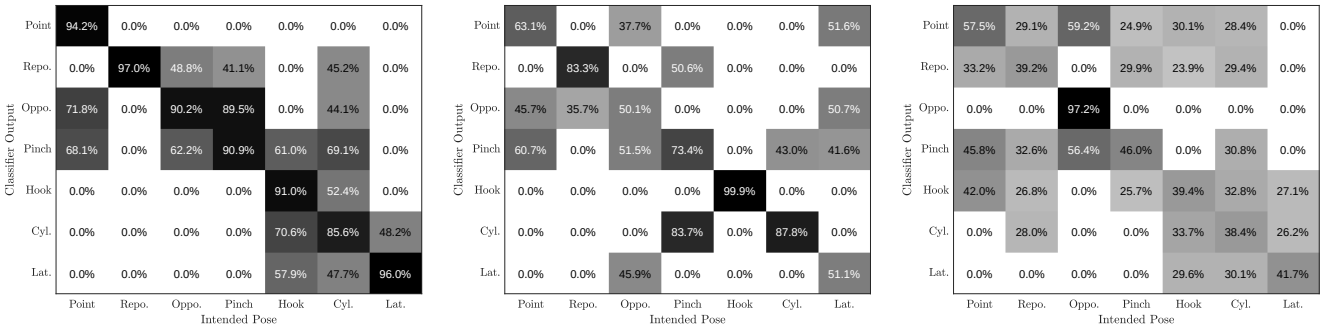

Fig. 6. Average confidence values for each classification for SCI participants show reduced performance as compared to able-bodied participants. However, the performance of the first participant (left) as well as the relatively high confidences for many of the diagonal (correct) values suggest that the proposed method still bears promise for use.

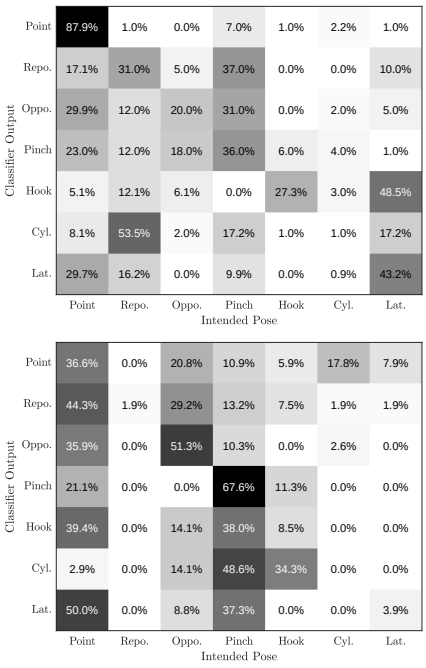

Fig. 7. Confusion matrices for SCI02 (left) and SCI03 (right) from the real time pilot study. The reduced performance likely arose from difficulties in real-time EMG segmentation, and identifies future work.

time implementation of the algorithm, may have been too coarsely segmented to provide a quality training set.

5.4 Future Work

Beyond the suggested improvements to the muscle activation measurement methods, additional sensors, or pose taxonomy discussed in Section 5, future work should center around studies using the SPAR Glove. First, these studies will clarify the impact of wearing the device on EMG patterns. While it is expected these patterns would change for able-bodied individuals, for the SCI participants who were unable to generate motion, the effects of wearing the SPAR Glove are unclear. Second, it will be straightforward to determine whether the low accuracies in the pilot study could be rectified with feedback from the classifier in the form of motion supported by the SPAR Glove, or if there are any additional challenges that may arise due to the movement of the hand. Finally, the combination of the validated algorithm with the SPAR Glove supporting motion could be validated through tasks aimed to evaluate participants' ability to perform ADL, with tests such as the SHAP described by Light et al. (2002).

These results also suggest future work for the intent detection algorithm. Improvements to the RMS-based segmentation strategy could avoid inadvertently captured periods of activity where the wearer is not initiating a pose, but instead maintaining a pose, or resetting to a neutral pose. Additionally, the relative weights of the nine parameters (Section 2.2) used by the classifier could be adjusted in addition to the retraining for each participant, potentially improving the performance over the standard set used for all participants in the experiment and pilot study. The IMU in the MYO may be leveraged here to provide additional input channels to act as either a triggering mechanism or as a way to account for compensatory movements which may be unique to each user.

6. CONCLUSION

This manuscript presented the details and experimental validation of the intent detection subsystem of the SPAR Glove, which uses a low-cost, wearable EMG system to detect the muscle activation patterns associated with one of seven goal poses. The accuracy rates for each able-bodied participant demonstrate the classifier's ability to recognize goal poses. There is a clear difference in the classifier's ability to correctly identify poses in the able-bodied versus the SCI population, but the data from the SCI participants demonstrate that classification is possible using only the data from the MYO armband. Future work aims to improve the performance of the proposed intent detection algorithm in a real-time implementation.

REFERENCES

Bennett, D.A. and Goldfarb, M. (2017). Imu-based wrist rotation control of a transradial myoelectric prosthesis. *IEEE Trans. on Neural Systems and Rehabilitation Engineering*, 26(2), 419–427.

Cai, L.L. et al. (2006). Implications of assist-as-needed robotic step training after a complete spinal cord injury on intrinsic strategies of motor learning. *J. of Neuroscience*, 26(41), 10564–10568.

Cao, H. and Zhang, D. (2016). Soft robotic glove with integrated semg sensing for disabled people with hand paral-

ysis. In *IEEE Intl. Conf. on Robotics and Biomimetics (ROBIO)*, 714–718.

Chu, C.Y. and Patterson, R.M. (2018). Soft robotic devices for hand rehabilitation and assistance: a narrative review. *J. of NeuroEngineering and Rehabilitation*, 15(9).

Collinger, J.L. et al. (2013). Functional priorities, assistive technology, and brain-computer interfaces after spinal cord injury. *J. of Rehabilitation Research and Development*, 50(2), 145.

Conti, R. et al. (2017). Development, design and validation of an assistive device for hand disabilities based on an innovative mechanism. *Robotica*, 35(4), 892–906.

Dalley, S.A., Varol, H.A., and Goldfarb, M. (2011). A method for the control of multigrasp myoelectric prosthetic hands. *IEEE Trans. on Neural Systems and Rehabilitation Engineering*, 20(1), 58–67.

Delph, M.A. et al. (2013). A soft robotic exomusculature glove with integrated semg sensing for hand rehabilitation. In *IEEE Intl. Conf. on Rehabilitation Robotics*.

Dietz, V. and Fouad, K. (2014). Restoration of sensorimotor functions after spinal cord injury. *Brain*, 137(3), 654–667.

Dietz, V., Muller, R., and Colombo, G. (2002). Locomotor activity in spinal man: significance of afferent input from joint and load receptors. *Brain*, 125(12), 2626–2634.

Dijkers, M. (1997). Quality of life after spinal cord injury: a meta analysis of the effects of disablement components. *Spinal cord*, 35(12).

Dollar, A.M. (2014). Classifying human hand use and the activities of daily living. In *The Human Hand as an Inspiration for Robot Hand Development*, 201–216. Springer.

Dwivedi, A. et al. (2019). A soft exoglove equipped with a wearable muscle-machine interface based on forcemyography and electromyography. *IEEE Robotics and Automation Letters*, 4(4), 3240–3246.

Edgerton, V.R. et al. (2004). Plasticity of the spinal neural circuitry after injury. *Annu. Rev. Neurosci.*, 27, 145–167.

Fougner, A. et al. (2012). Control of upper limb prostheses: terminology and proportional myoelectric control—a review. *IEEE Trans. on neural systems and rehabilitation engineering*, 20(5), 663–677.

Gailey, A., Artemiadis, P., and Santello, M. (2017). Proof of concept of an online emg-based decoding of hand postures and individual digit forces for prosthetic hand control. *Frontiers in neurology*, 8, 7.

Hudgins, B., Parker, P., and Scott, R.N. (1993). A new strategy for multifunction myoelectric control. *IEEE Trans. on biomedical engineering*, 40(1), 82–94.

In, H. et al. (2015). Exo-glove: a wearable robot for the hand with a soft tendon routing system. *IEEE Robotics & Automation Magazine*, 22(1), 97–105.

Jeong, U., In, H.K., and Cho, K.J. (2013). Implementation of various control algorithms for hand rehabilitation exercise using wearable robotic hand. *Intelligent Service Robotics*, 6(4), 181–189.

Johanson, M.E. and Murray, W.M. (2002). The unoperated hand: the role of passive forces in hand function after tetraplegia. *Hand clinics*, 18(3), 391–398.

Kadowaki, Y. et al. (2011). Development of soft power-assist glove and control based on human intent. *J. of Robotics and Mechatronics*, 23(2), 281–291. doi:10.20965/jrm.2011.p0281.

Kristensen, H.K. et al. (2011). Evaluation of evidence within occupational therapy in stroke rehabilitation. *Scandinavian journal of occupational therapy*, 18(1), 11–25.

Light, C.M., Chappell, P.H., and Kyberd, P.J. (2002). Establishing a standardized clinical assessment tool of pathologic and prosthetic hand function: normative data, reliability, and validity. *Archives of physical medicine and rehabilitation*, 83(6), 776–783.

Losey, D.P. et al. (2018). A review of intent detection, arbitration, and communication aspects of shared control for physical human–robot interaction. *Applied Mechanics Reviews*, 70(1).

Maciejasz, P. et al. (2014). A survey on robotic devices for upper limb rehabilitation. *J. of neuroengineering and rehabilitation*, 11(1), 3.

McDonald, C.G. et al. (2020). A myoelectric control interface for upper-limb robotic rehabilitation following spinal cord injury. *IEEE Trans. on Neural Systems and Rehabilitation Engineering*, 28(4), 978–987.

Mendez, I. et al. (2017). Evaluation of the myo armband for the classification of hand motions. In *2017 Intl. Conf. on Rehabilitation Robotics (ICORR)*, 1211–1214. IEEE.

National Spinal Cord Injury Statistical Center (2017). Spinal cord injury facts and figures at a glance. *University of Alabama at Birmingham*.

Ochoa, J.M. et al. (2011). Use of an electromyographically driven hand orthosis for training after stroke. In *2011 IEEE Intl. Conf. on Rehabilitation Robotics*, 1–5. IEEE.

Pezent, E. and McDonald, C.G. (2019). Github - mahilab/MEL: Mechatronics Engine & Library. https://github.com/mahilab/MEL. (accessed: 18.01.2019).

Piovanelli, E., Piovesan, D., Shirafuji, S., Su, B., Yoshimura, N., Ogata, Y., and Ota, J. (2020). Towards a simplified estimation of muscle activation pattern from mri and emg using electrical network and graph theory. *Sensors*, 20(3), 724.

Polygerinos, P. et al. (2015). Emg controlled soft robotic glove for assistance during activities of daily living. In *Rehabilitation Robotics (ICORR), 2015 IEEE Intl. Conf. on*, 55–60. IEEE.

Rose, C.G. and O'Malley, M.K. (2019). Hybrid rigid-soft hand exoskeleton to assist functional dexterity. *IEEE Robotics and Automation Letters*, 4(1), 73–80.

Santello, M., Flanders, M., and Soechting, J.F. (1998). Postural hand synergies for tool use. *J. of Neuroscience*, 18(23), 10105–10115.

Shanechi, M.M. (2017). Brain–machine interface control algorithms. *IEEE Trans. on Neural Systems and Rehabilitation Engineering*, 25(10), 1725–1734.

Triandafilou, K.M. et al. (2011). Transient impact of prolonged versus repetitive stretch on hand motor control in chronic stroke. *Topics in stroke rehabilitation*, 18(4), 316–324.

Winstein, C.J., Merians, A.S., and Sullivan, K.J. (1999). Motor learning after unilateral brain damage. *Neuropsychologia*, 37(8), 975–987.

Xu, Z., Shen, L., Qian, J., and Zhang, Z. (2020). Advanced hand gesture prediction robust to electrode shift with an arbitrary angle. *Sensors*, 20(4), 1113.